Microstrip Dispersion Including Anisotropic Substrates

BRIAN E. KRETCH, MEMBER, IEEE, AND ROBERT E. COLLIN, FELLOW, IEEE

Abstract — **A perturbation-iteration solution based on potential theory is developed for determining the effective dielectric constant, characteristic impedance, and current–charge distribution on a microstrip transmission line with isotropic and anisotropic substrates. The numerical implementation of the theory is described and is suitable for use on a personal computer. Computed data for several common substrate materials are included.**

I. Introduction

THE DISPERSIVE properties of microstrip transmission lines have been described by a number of authors, and this includes some work on anisotropic substrates as well. A very popular approach is based on the expansion of the fields in terms of hybrid (longitudinal section) modes, the formulation of an integral equation in terms of the unknown currents on the strip, and the solution of the equation in the spectral domain using Galerkin's method [1]–[5]. For comprehensive reviews, see [6] and [7]. This approach requires finding the roots of a transcendental dispersion equation. For wide strips, the modified Wiener–Hopf technique can be utilized quite effectively [8]. The analysis of microstrip lines has also been carried out using potential theory [9]–[11].

In this paper, we present a new perturbation-iteration solution based on potential theory that leads to a very efficient computation of the dispersive properties of a microstrip line on isotropic or anisotropic substrates. The initial development of the perturbation-iteration solution for isotropic substrates was carried out as a thesis project [12], [13] (an unfortunate sign error in the computer program makes the numerical results given in [12] and [13] increasingly inaccurate as the frequency is increased). The theory presented in this paper is an improved version and is also generalized to allow for anisotropic substrates. Our potential theory includes the use of all three components of the vector potential function, and this leads to a number of simplifications in the final pair of uncoupled scalar integral equations that must be solved.

Manuscript received October 14, 1986; revised April 11, 1987. This work was supported in part by NASA Lewis Research Center, Cleveland, OH, under Grant NCC 3-29

B. E. Kretch is with the Federal Systems Division, IBM Corporation, Gaithersburg, MD 20879.

R. E. Collin is with Case Western Reserve University, Cleveland, OH, 44106.

IEEE Log Number 8715414.

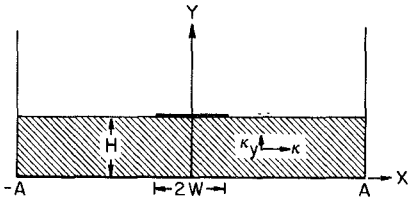

Fig. 1. A microstrip transmission line.

II. Field Equations

The microstrip line under consideration is shown in Fig. 1. It consists of a conducting strip of width $2W$ located on a substrate of thickness H on a ground plane. Two conducting sidewalls are placed at $x = \pm A$ in order to facilitate the analysis through use of Fourier series. When numerical results are computed, A is set equal to the larger of $15W$ or $15H$, for which case the sidewalls have a negligible influence on the characteristics of the microstrip line. The substrate is assumed to be anisotropic with a dielectric constant κ_y in the direction perpendicular to the substrate and κ in the x and z directions. All field quantities have a time dependence $e^{j\omega t}$ and a z dependence $e^{-j\beta z}$ and these common factors are suppressed after the basic equations have been developed.

The equations for the vector and scalar potentials are developed initially by letting κ_y and κ be functions of y. An important feature of this approach is that it requires the vector potential $\boldsymbol{A}$ to have all three components A_x, A_y, A_z. In addition, we keep the scalar potential Φ as an explicit part of the solution. By including an A_y component, all of the potential functions can be continuous across the air–dielectric interface. In the potential theory referred to earlier, A_y is chosen as zero with the consequence that the potentials must all be discontinuous across the air–dielectric interface [9]–[11]. Thus, the potential theory that we use is a more natural one and leads to a very efficient iterative theory for evaluating microstrip dispersion. It also has the advantage of eliminating the coupling between A_z and Φ at the air–dielectric interface.

The dielectric constant tensor is represented as

$$\bar{\kappa}(y) = \kappa(y)\bar{I} + \left[\kappa_y(y) - \kappa(y)\right]\boldsymbol{a}_y\boldsymbol{a}_y \tag{1}$$

where $\bar{I}$ is the unit dyad. We let $\boldsymbol{B} = \nabla \times \boldsymbol{A}$ and then from Maxwell's equation $\nabla \times \boldsymbol{E} = -j\omega\nabla \times \boldsymbol{A}$ we obtain

$$\boldsymbol{E} = -j\omega\boldsymbol{A} - \nabla\Phi. \tag{2}$$

From the equation $\nabla \times \boldsymbol{B} = j\omega\mu_0\epsilon_0\bar{\kappa}\cdot\boldsymbol{E} + \mu_0\boldsymbol{J} = \nabla \times \nabla \times \boldsymbol{A}$ we find, upon using (2), that

$$\begin{aligned}\nabla\nabla\cdot\boldsymbol{A} - \nabla^2\boldsymbol{A} &= j\omega\epsilon_0\mu_0\big[-j\omega\kappa\boldsymbol{A} - \kappa\nabla\Phi - j\omega(\kappa_y-\kappa)\\ &\quad\cdot A_y\boldsymbol{a}_y - (\kappa_y-\kappa)\nabla\Phi\cdot\boldsymbol{a}_y\boldsymbol{a}_y\big] + \mu_0\boldsymbol{J}\\ &= \kappa k_0^2\boldsymbol{A} - j\omega\mu_0\epsilon_0\nabla(\kappa\Phi)\\ &\quad -(\kappa_y-\kappa)\left(j\omega\mu_0\epsilon_0\frac{\partial\Phi}{\partial y} - k_0^2A_y\right)\boldsymbol{a}_y\\ &\quad + j\omega\mu_0\epsilon_0\Phi\frac{\partial\kappa}{\partial y}\boldsymbol{a}_y + \mu_0\boldsymbol{J}.\end{aligned}$$

The two gradient terms are now equated to yield the conventional Lorentz condition and the following equations for the components of $\boldsymbol{A}$:

$$\nabla\cdot\boldsymbol{A} = -j\omega\mu_0\epsilon_0\kappa(y)\Phi \tag{3a}$$

$$\nabla^2A_z + \kappa k_0^2A_z = -\mu_0J_z \tag{3b}$$

$$\nabla^2A_x + \kappa k_0^2A_x = -\mu_0J_x \tag{3c}$$

$$\nabla^2A_y + \kappa_y k_0^2A_y = -j\omega\mu_0\epsilon_0\Phi\frac{\partial\kappa}{\partial y} + j\omega\mu_0\epsilon_0(\kappa_y-\kappa)\frac{\partial\Phi}{\partial y}$$

$$= j\omega\mu_0\epsilon_0\left[(\kappa_y-\kappa)\frac{\partial\Phi}{\partial y} + \Phi(H)(\kappa-1)\delta(y-H)\right] \tag{3d}$$

where we have taken the step change in $\kappa(y)$ at $y=H$ into account and put $\partial\kappa/\partial y = (1-\kappa)\delta(y-H)$, with $\delta(y-H)$ being the delta function. By using Gauss's law $\nabla\cdot(\bar{\kappa}\cdot E) = \rho/\epsilon_0$, (2), and the Lorentz condition, the following equation for Φ is obtained

$$\kappa\left[\frac{\partial^2\Phi}{\partial x^2} + \frac{\partial^2\Phi}{\partial z^2}\right] + \frac{\partial}{\partial y}\kappa_y\frac{\partial\Phi}{\partial y} + \kappa^2k_0^2\Phi$$

$$= -\frac{\rho}{\epsilon_0} + j\omega(\kappa_y-1)\delta(y-H)A_y - j\omega(\kappa_y-\kappa)\frac{\partial A_y}{\partial y}. \tag{4}$$

In (3) J_x and J_z are the components of the current density on the microstrip, and in (4) ρ is the charge density. At the air–dielectric interface, all of the potential functions are continuous across the interface. In addition, $\partial A_x/\partial y$ and $\partial A_z/\partial y$ are also continuous across the interface. From the differential equations (3d) and (4) we find, by integrating over a vanishingly small interval along y centered on the interface, that

$$\left.\frac{\partial A_y}{\partial y}\right|_-^+ = j\omega\mu_0\epsilon_0(\kappa-1)\Phi(H) \tag{5a}$$

$$\left.\kappa_y(y)\frac{\partial\Phi}{\partial y}\right|_-^+ = \left.\frac{\partial\Phi}{\partial y}\right|_+ - \kappa_y\left.\frac{\partial\Phi}{\partial y}\right|_-$$

$$= -\frac{\rho}{\epsilon_0} + j\omega(\kappa_y-1)A_y(H) \tag{5b}$$

where the negative sign refers to y just below the interface and the postive sign refers to y just above the conducting strip. In addition to these discontinuity conditions, the boundary conditions on the perfectly conducting infinitely thin microstrip are

$$E_z = 0 \text{ or } \omega A_z = \beta\Phi \tag{6a}$$

$$E_x = 0 \text{ or } -j\omega A_x = \frac{\partial\Phi}{\partial x}. \tag{6b}$$

One additional relationship that will be used comes from integrating the continuity equation

$$\nabla_s\cdot\boldsymbol{J} = -j\omega\rho$$

across the strip from $x = -W$ to W; it is

$$\beta I_{\text{TOT}} = \omega Q \tag{7}$$

where I_{TOT} is the total z-directed current and Q is the total charge per unit length on the strip.

The integral of (6b) on the strip gives

$$\Phi(x,H) = -j\omega\int_0^x A_x\,dx + \Phi(0,H)$$

which can be expressed in the form

$$\epsilon_0\Phi(x,H) = 1 - j\omega\mu_0\epsilon_0\int_0^x\int_{-W}^{W}G(x,x')J_x(x')\,dx'\,dx \tag{8}$$

for $0 < x < W$. In (8) we have set $\Phi(0,H)$ equal to $1/\epsilon_0$. The second term in (8), involving the integral of J_x and the Green's function G for (3c), is a small perturbation to the boundary condition for Φ since at the lower frequencies, and in particular for narrow strips, J_x is very small. Numerical computations show that even for extreme conditions this term is not large. For example, for $H=1$ mm, $\kappa = \kappa_y = 10$, and $2W = 10H$, this term represents no more than a 50-percent decrease in the value of Φ from $x=0$ to $x=W$ at 26 GHz. For all practical microstrip lines within the useful frequency range, it is a much smaller perturbation term and is treated as such in the iteration-perturbation theory that is developed in this paper. For $2W/H = 6$ and $\kappa = 12$, J_x causes an 8-percent decrease in Φ at $x=W$ for $f=10$ GHz. For narrower strips and smaller values of the dielectric constant, the decrease is less. For $2W/H < 1$, the effect of J_x can be neglected, even at 20 GHz for $H=1$ mm.

III. Formal Solution

The current J_z and charge ρ can be represented by the following Fourier series:

$$J_z(x) = \sum_{n=1,3\cdots}^{\infty} J_n\cos w_nx \tag{9a}$$

$$\rho(x) = \sum_{n=1,3\cdots}^{\infty} \rho_n\cos w_nx \tag{9b}$$

where

$$J_n = \frac{2}{a}\int_0^1 J_z(x)\cos w_nx\,dx \tag{10a}$$

$$\rho_n = \frac{2}{a}\int_0^1 \rho(x)\cos w_nx\,dx. \tag{10b}$$

At this point normalized dimensions have been introduced so that $W = 1$m, $a = A/W$, and $\alpha = H/W$. Also, $w_n =$

$n\pi/2a$ in (9) and (10). The potentials are also represented by Fourier series in the form

$$\Phi = \sum_{n=1,3\cdots}^{\infty} \Phi_n(y)\cos w_n x \tag{11a}$$

$$A_z = \sum_{n=1,3\cdots}^{\infty} A_{zn}(y)\cos w_n x \tag{11b}$$

$$A_y = \sum_{n=1,3\cdots}^{\infty} A_{yn}(y)\cos w_n x \tag{11c}$$

$$A_x = \sum_{n=1,3\cdots}^{\infty} A_{xn}(y)\sin w_n x \tag{11d}$$

where the factor $e^{-j\beta z}$ has now been suppressed. The equations for Φ and A_y must be solved simultaneously. In view of the boundary conditions that must hold at $y=0$, we can assume that

$$\Phi_n = C\sinh\gamma y \qquad A_{yn} = D\cosh\gamma y \qquad y<\alpha$$

and substitute these into (3d) and (4). It is then readily found that solutions exist for two values of γ given by

$$\gamma_{1n} = \left(\beta^2 - \kappa k_0^2 + w_n^2\right)^{1/2} \tag{12a}$$

$$\gamma_{2n} = \left(\frac{\kappa}{\kappa_y}\right)^{1/2}\left(\beta^2 - \kappa_y k_0^2 + w_n^2\right)^{1/2}. \tag{12b}$$

The general solutions for Φ_n and A_{yn} are now chosen as

$$\Phi_n = \begin{cases} C_1\sinh\gamma_{1n}y + C_2\sinh\gamma_{2n}y, & y\leqslant\alpha \\ C_3 e^{-\gamma_n y}, & y\geqslant\alpha \end{cases}$$

$$A_{yn} = \begin{cases} D_1\cosh\gamma_{1n}y + D_2\cosh\gamma_{2n}y, & y\leqslant\alpha \\ D_3 e^{-\gamma_n y}, & y\geqslant\alpha \end{cases}$$

where

$$\gamma_n = \left(\beta^2 - k_0^2 + w_n^2\right)^{1/2}.$$

The potentials are continuous at $y=\alpha$ and satisfy the discontinuity conditions given by (5). The use of these boundary conditions and the requirement that the solutions satisfy the coupled differential equations lead to the solution

$$\epsilon_0\Phi_n(\alpha) = \left[\frac{w_1(n)w_3(n)\,\mathrm{Sh}_3(n)}{w_3(n)\,\mathrm{Sh}_3(n) + \kappa w_1(n)\,\mathrm{Ch}_3(n)} + \frac{k_0^2\,\mathrm{Sh}_2(n)}{w_1(n)\,\mathrm{Sh}_2(n) + w_2(n)\,\mathrm{Ch}_2(n)}\right]\frac{\rho_n}{\beta^2 + w_n^2} \tag{13}$$

where the following shorthand notation has been introduced:

$$w_1(n) = \gamma_n \qquad \mathrm{Sh}_i(n) = \sinh w_i(n)\alpha$$
$$w_2(n) = \gamma_{1n} \qquad \mathrm{Ch}_i(n) = \cosh w_i(n)\alpha$$
$$w_3(n) = \gamma_{3n} \qquad i = 1,2,3.$$

We also use

$$\beta^2 = \kappa_e k_0^2 \tag{14}$$

where κ_e is the effective dielectric constant. The coefficient of ρ_n in (13) is the nth coefficient of the Green's function G_2 needed to solve for Φ in terms of ρ after eliminating A_y. When $k_0 = 0$, we have

$$\epsilon_0\Phi_n(\alpha) = \frac{\rho_n \sinh w_n\alpha'}{w_n\left(\sinh w_n\alpha' + \sqrt{\kappa\kappa_y}\cosh w_n\alpha'\right)} \tag{15}$$

where $\alpha' = (\kappa/\kappa_y)^{1/2}\alpha$. The result shown in (15) expresses the property that the potential Φ for an anisotropic substrate is the same as that for an isotropic substrate with dielectric constant $(\kappa\kappa_y)^{1/2}$ and normalized thickness α'[14]. However, A_z is still the same as for a line with normalized height α for the strip, so the zero frequency inductance per unit length must be found for the unscaled line. This can be expressed in terms of the capacitance of the air-filled unscaled line.

The solution for A_{zn} is much easier to find and is, at $y=\alpha$,

$$A_{zn} = \frac{\mu_0 J_{zn}\,\mathrm{Sh}_2(n)}{w_1(n)\,\mathrm{Sh}_2(n) + w_2(n)\,\mathrm{Ch}_2(n)} \tag{16}$$

which reduces, for $k_0 = 0$, to

$$A_{zn} = \mu_0 J_{zn} e^{-w_n\alpha}\frac{\sinh w_n\alpha}{w_n}. \tag{17}$$

The coefficient of $\mu_0 J_{zn}$ is the nth Fourier coefficient of the Green's function G_1 needed to solve for A_z in terms of J_z.

At $y=\alpha$, the Green's functions G_1 and G_2 have the representations

$$G_i(x,x') = \frac{1}{a}\sum_{n=1,3\cdots}^{\infty} G_{in}\cos w_n x\cos w_n x', \qquad i=1,2, \tag{18}$$

where G_{1n} is the coefficient of $\mu_0 J_{zn}$ in (16) or (17) and G_{2n} is the coefficient of ρ_n in (13) or (15).

The Fourier series solution for A_x can be found directly from the Lorentz condition (3a), so J_x does not need to be solved for explicitly. An alternative procedure is to use the continuity equation to find J_x.

IV. Static Green's Functions

In the iteration solution to be presented in the next section, we will need the static Green's functions G_1^0 and G_2^0. In this section, we sum the dominant or the singular part of the series for the G_i^0 into closed form, which can then later be integrated exactly as the dominant part of the integral equations that will be set up for ρ and J_z.

The static Green's function G_1^0, at $y=\alpha$, is given by

$$G_1^0(x,x') = \sum_{n=1,3\cdots}^{\infty}\frac{2\cos w_n x\cos w_n x'(1-e^{-2w_n\alpha})}{n\pi}. \tag{19}$$

The two series can be summed to give [15]

$$G_1^0 = -\frac{1}{4\pi}\ln\left(\tan\frac{\pi}{4a}|x-x'|\tan\frac{\pi}{4a}|x+x'|\right) - \frac{1}{8\pi}\ln\left\{\left[\frac{\cosh\frac{\pi\alpha}{a}+\cos\frac{\pi}{2a}(x-x')}{\cosh\frac{\pi\alpha}{a}-\cos\frac{\pi}{2a}(x-x')}\,\frac{\cosh\frac{\pi\alpha}{a}+\cos\frac{\pi}{2a}(x+x')}{\cosh\frac{\pi\alpha}{a}-\cos\frac{\pi}{2a}(x+x')}\right]\right\}. \quad (20)$$

We now assume that a is set equal to the larger of 15 or 15α, in which case α/a and $(x \pm x')/a$ are small. Hence, we can use the small argument approximations for the cosine and hyperbolic cosine terms and also expand the logarithm to obtain

$$G_1^0 = -\frac{1}{4\pi}\ln|x^2-x'^2| + \frac{1}{8\pi}\ln\left\{\left[(2\alpha)^2+(x-x')^2\right]\left[(2\alpha)^2+(x+x')^2\right]\right\} - \frac{\pi\alpha^2}{24a^2}. \quad (21)$$

The dominant term in α/a has been retained in (21) in order to determine how large a has to be before the sidewalls have a negligible effect. The numerical results verify the condition given after (20).

The static Green's function G_2^0 at $y=\alpha$ is given by

$$G_2^0(x,x') \sum_{n=1,3\cdots}^{\infty} \frac{2\cos w_n x\cos w_n x'\sinh w_n\alpha'}{n\pi\left(\sinh w_n\alpha' + \kappa_g\cosh w_n\alpha'\right)} \quad (22)$$

where $\kappa_g = (\kappa\kappa_y)^{1/2}$ and $\alpha' = (\kappa/\kappa_y)^{1/2}\alpha$. The above series may be expressed in the form

$$G_2^0(x,x') = \sum_{n=1,3\cdots}^{\infty} \frac{2\cos w_n x\cos w_n x'(1-e^{-2w_n\alpha'})}{(\kappa_g+1)n\pi(1+\eta e^{-2w_n\alpha'})}$$

where $\eta = (\kappa_g-1)/(\kappa_g+1)$. We now expand the factor $(1+\eta e^{-2w_n\alpha'})^{-1}$ into a power series and can then carry out the summation over n for each term to obtain

$$G_2^0(x,x') = \frac{2}{\kappa_g+1}G_1^0(x,x',\alpha') - \frac{\kappa_g}{2\pi(\kappa_g+1)^2}\left\{\frac{\kappa_g-1}{2\kappa_g}\cdot\ln\left[\frac{\cosh\frac{\pi\alpha'}{a}+\cos\frac{\pi}{2a}(x-x')}{\cosh\frac{\pi\alpha'}{a}-\cos\frac{\pi}{2a}(x-x')}\right]\right.$$
$$\times\left[\frac{\cosh\frac{\pi\alpha'}{a}+\cos\frac{\pi}{2a}(x+x')}{\cosh\frac{\pi\alpha'}{a}-\cos\frac{\pi}{2a}(x+x')}\right] + \sum_{m+1}^{\infty}(-\eta)^m\ln\left[\frac{\cosh(m+1)\frac{\pi\alpha'}{a}+\cos\frac{\pi}{2a}(x-x')}{\cosh(m+1)\frac{\pi\alpha'}{a}-\cos\frac{\pi}{2a}(x-x')}\right]$$
$$\left.\times\left[\frac{\cosh(m+1)\frac{\pi\alpha'}{a}+\cos\frac{\pi}{2a}(x+x')}{\cosh(m+1)\frac{\pi\alpha'}{a}-\cos\frac{\pi}{2a}(x+x')}\right]\right\}. \quad (23)$$

The alternating series represents a correction to the dominant part of G_2^0 which is expressed in closed form. In the numerical evaluation of the integral involving G_2^0, it was established that truncating the series when the mth term was smaller than 10^{-3} times the sum of the first $m-1$ terms resulted in an insignificant error. For narrow strips with κ_g less than 5, it is found that 8 to 10 terms are sufficient, while for strips as wide as $10H$ and with $\kappa_g = 12$, a total of 45 terms were required.

V. Solution by Iteration

In the iteration method the current and charge densities and the effective dielectric constant κ_e are first found at zero frequency. For this case $\epsilon_0\Phi$ is set equal to 1 on the strip, and A_{zr}/μ_0 is also set equal to 1 on the strip, where A_{zr} is a reference value for the vector potential. The integral equations to be solved are

$$2\int_0^1 G_1^0(x,x')J_{zr}(x')\,dx' = 1 \quad (24a)$$

$$2\int_0^1 G_2^0(x,x')\rho(x')\,dx' = 1. \quad (24b)$$

The current J_z is expanded in terms of four basis functions in the form

$$J_z = \frac{I_0 - I_1T_2(x) + I_2T_4(x) - I_3T_6(x)}{\sqrt{1-x^2}} \quad (25)$$

where $T_n(x)$ is a Chebyshev polynomial. A simple equivalent power series in x^{2n} was also tried but the resultant matrix was ill conditioned in that case. By using the Chebyshev polynomials, the matrix determinant was larger by a factor of about 100. In the numerical evaluation, the substitution $x = \sin\theta$ is made, in which case

$$J_z(x)\,dx = (I_0 + I_1\cos 2\theta + I_3\cos 4\theta + I_4\cos 6\theta)\,d\theta. \quad (26)$$

A similar expansion for ρ is used with coefficients Q_n, $n = 0,1,2,3$.

By using the above expansion and substitution, we can use the Schwinger transformation

$$\ln|x^2-x'^2| = \ln|\sin^2\theta-\sin^2\theta'| = \ln\left|\frac{\cos 2\theta-\cos 2\theta'}{2}\right|$$
$$= -\ln 4 - \sum_{n=1}^{\infty}\frac{2\cos 2n\theta\cos 2n\theta'}{n} \tag{27}$$

which enables one to carry out the integrals in (24) analytically for the dominant parts of G_1^0 and G_2^0. The remaining integrals are evaluated numerically. Equations (24) are converted to matrix equations by using point matching at the four points $x=\sin(2i+1)\pi/16$, $i=0,1,2,3$. Test cases using Galerkin's method and the method of least squares were also evaluated with essentially the same results, so the final computer program adopted used point matching since it requires somewhat less computational effort. The numerical results show that I_2 and Q_2 are small and I_3 and Q_3 are almost negligible so four basis functions are sufficient.

After the expansion coefficients I_n and Q_n for ρ have been found, the total current and charge on the strip are given by $I_T=\pi I_0$ and $Q_T=\pi Q_0$. The total current is a relative value, so we now multiply I_T by a constant K and enforce the two conditions (6a) and (7) to obtain

$$\omega\epsilon_0 KA_{zr} = \beta\epsilon_0\Phi = \beta = \omega\mu_0\epsilon_0 K$$

and

$$\beta K I_T = \omega Q_T$$

which then gives

$$\frac{\beta^2}{k_0^2} = \kappa_e = \frac{Q_T}{I_T} \tag{28}$$

$$Z_0 = \frac{1/\epsilon_0}{KI_T} = \frac{Z}{I_T\sqrt{\kappa_e}} \tag{29}$$

where $Z=(\mu_0/\epsilon_0)^{1/2}=120\pi\ \Omega$ and $\beta K=\omega\kappa_e$.

The next step that is carried out is to evaluate the Fourier coefficients J_{zn} and ρ_n using the static current and charge distributions. The Green's functions at the first frequency increment (typically we use steps of 1 GHz or 2 GHz) are approximated by using the static value of κ_e, and the following integral equations are solved:

$$2\int_0^1 G_1^1(x,x')J_{zr}(x')\,dx' = 1+S(x) \tag{30a}$$

$$2\int_0^1 G_2^1(x,x')\rho(x')\,dx' = 1+S(x) \tag{30b}$$

where $S(x)$ is the correction to the static boundary value for the potentials as given by (8). From the continuity equation, we obtain

$$w_n J_{xn} = j\omega(\kappa_e J_{zn}-\rho_n).$$

Also, the Green's function for A_x has the same Fourier coefficients G_{1n} but with $\sin w_n x$ replacing $\cos w_n x$. By using these relations, the integral in (8) is readily evaluated to give

$$S(x) = \sum_{n=1,3,\cdots} G_{1n}^0\frac{\cos w_n x-1}{w_n^2}(\rho_n-\kappa_e J_{zn}). \tag{31}$$

Note that $\rho_n-\kappa_e J_{zn}$ is proportional to the nth Fourier coefficient of J_x and is therefore quite small. The Green's functions G_1^1 and G_2^1 at the first iteration (denoted by the superscript 1) are expressed as

$$G_i^1 = G_i^0 + (G_i^1 - G_i^0).$$

The first part is the static Green's function or dominant part, while the second part is a correction and is represented in a Fourier series form. By means of this technique, it turns out that good numerical convergence is obtained by using only 30 terms in the Fourier series for the correction term and also for $S(x)$. The integral equations in (30) are solved, and new values of I_n and Q_n at the first frequency increment are thus obtained. A corrected value of κ_e may then be found using the same relation given earlier by (28).

The iteration is now repeated by calculating a more accurate value for $S(x)$ using the new value of κ_e and new computed values for ρ_n and J_{zn}. The new value of κ_e is also used in the Green's function G_1^2 and G_2^2 for the second iteration. These Green's functions are expressed in the form

$$G_i^2 = G_i^1 + (G_i^2 - G_i^1).$$

The first term is known from the earlier computation and the second term is a rapidly converging Fourier series correction term. This iteration procedure is repeated until successive values of κ_e do not change by more than 0.1 percent. When convergence has been obtained, the frequency is incremented to the next value. Linear extrapolation is used to obtain a good initial value for κ_e at the new frequency. By this means, the iteration converges very fast, and typically 1, 2, or 3 iterations are all that is required at each frequency when the frequency increment is 2 GHz. A smaller frequency increment requires fewer iterations at each new frequency.

At each frequency, the characteristic impedance of the microstrip line is evaluated after a converged value of κ_e has been found. The following definition for the characteristic impedance Z_0 is used:

$$Z_0 = \frac{1}{I_{\mathrm{TOT}}}\int_0^{\alpha} -E_y\,dy = \frac{1}{I_T}\left[\int_0^{\alpha}\left(\frac{\partial\Phi}{\partial y}+j\omega A_y\right)dy\right]$$
$$= \frac{1}{I_{\mathrm{TOT}}}\left[\frac{1}{\epsilon_0}+j\omega\int_0^{\alpha}A_y\,dy\right] \tag{32}$$

where I_{TOT} is the total z-directed current on the strip, and the integral of E_y is carried out at $x=0$ to obtain an equivalent voltage across the line. The vector potential function A_y can be evaluated in Fourier series form so that (32) can be expressed as

$$Z_0 = \frac{120\pi}{I_T\sqrt{\kappa_e}}\left\{1+\sum_{n=1,3\cdots}\frac{k_0^2\rho_n}{\kappa_e k_0^2+w_n^2}\left[\frac{\kappa w_1(n)\,\mathrm{Sh}_3(n)}{w_3(n)[w_{3n}(n)\,\mathrm{Sh}_3(n)+\kappa w_1(n)\,\mathrm{Ch}_3(n)}-\frac{\mathrm{Sh}_2(n)}{w_1(n)\,\mathrm{Sh}_2(n)+w_2(n)\,\mathrm{Ch}_2(n)}\right]\right\} \tag{33}$$

where I_T is the total relative value of the z-directed current obtained from the solution of an equation like (30a) in the last iteration at the frequency of interest. A total of 30 terms gives an accurate value for the sum in (33).

A computer program written in BASIC was developed to implement the theory presented above. The techniques used, such as extracting the dominant parts of the Green's functions and evaluating the important parts of the integrals analytically, resulted in a robust and numerically efficient program. The program, when run on an ATT-6300 (clock frequency at 8 MHz) in compiled form, will completely characterize a given microstrip line with an anisotropic substrate (effective dielectric constant κ_e, characteristic impedance Z_0, current and charge expansion coefficients I_n, Q_n) in 2-GHz frequency steps from 0 to 30 GHz in less than 2 minutes. The numerical accuracy is ± 0.25 percent and only single precision arithmetic is required.

Most of the computations need to be done only once. For example, the sum over m in (23) is carried out only once. Likewise, the basic integrals

$$\int_0^{\pi/2} \cos(w_n \sin\theta)\cos 2i\theta \, d\theta, \qquad i = 0,1,2,3$$

for the Fourier coefficients need to be evaluated only once. These integrals were evaluated by quadrature, which is as efficient as expressing them in terms of Bessel functions and using Bessel function routines. Since the Green's functions are expressed in terms of those evaluated earlier plus correction series, they can also be evaluated with a minimum of computational time. All of these features contribute to the efficiency of the computer program. In the spectral-domain approach, very little analytical preprocessing of the formulas appears to be done, even though in principle the dominant parts of the Fourier transforms could be extracted and evaluated analytically. For programs that are to be run on personal computers, it is well worth the effort to do as much analytical simplification as possible since it compensates for the inherently slower speed of personal computers.

VI. Numerical Results

Kuester and Chang have shown that the numerical results for microstrip effective dielectric constant by various authors differ by significant amounts due to numerical approximations and limitations of the procedures used [16]. It is important to verify, as far as possible, the validity and accuracy of the numerical results obtained from a computer program.

We have checked our results against those given by Jansen [2] (Fig. 2 and Fig. 6 data) and they agree to within the accuracy that data can be read from the graphs, with the exception of the two narrowest strips considered by Jansen. For $2W/H = 0.0625$, our results for the effective dielectric constant are 3.5 to 4.5 percent larger. For $2W/H = 0.09375$, our results are 1.5 to 2.3 percent larger. We have checked our static values with Wheeler's formula and get agreement to better than 1 percent.

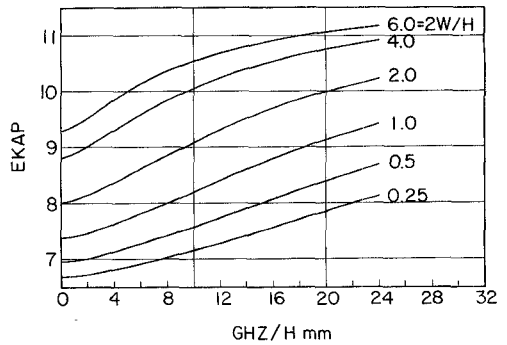

Fig. 2. Effective dielectric constant for a sapphire substrate

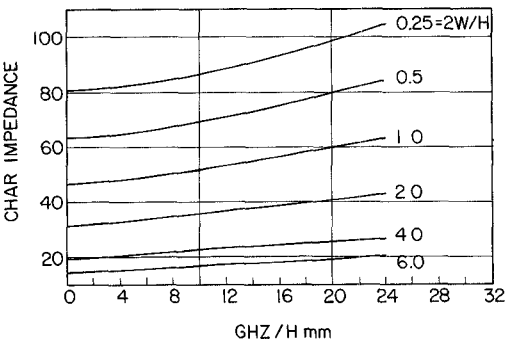

Fig. 3. Characteristic impedance with a sapphire substrate.

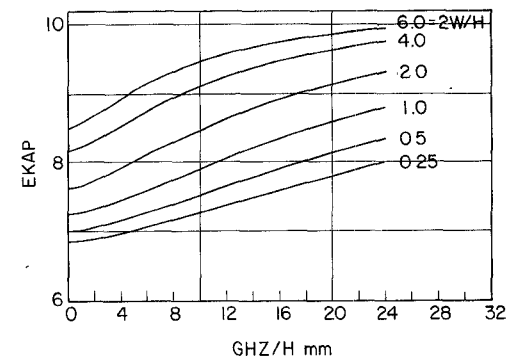

Fig. 4. Effective dielectric constant for Epsilam-10 substrate.

Our results also agree to within the accuracy of reading graphical data (better than 0.5 percent) with those of Kuester and Chang [10] (Figs. 2–5). For anisotropic substrates such as sapphire, our results agree very closely with those of El-Sherbiny [8] (Figs. 2–4). The results obtained by Kitazawa and Hayashi [4] show a small disagreement with those of El-Sherbiny for wide strips at the higher frequencies. Our results support those obtained by El-Sherbiny. The results for κ_e given by Tsalamengas *et al.* [17, table III, $\theta_0 = 0°$] for a sapphire substrate with $\kappa = 9.4$, $\kappa_y = 11.6$, and $2W/H = 2$ appear to be in error (too large) by about 5 percent at the lower frequencies. An extrapolation of their data to zero frequency does not give results that agree with the static values which are easy to compute with good accuracy [18]. Tsalamengas has recomputed the low-frequency values using more basis functions and has verified our low-frequency values, which at zero frequency agree with those obtained by Owens *et al.* [18]. Thus, based on the available published data, it is believed that

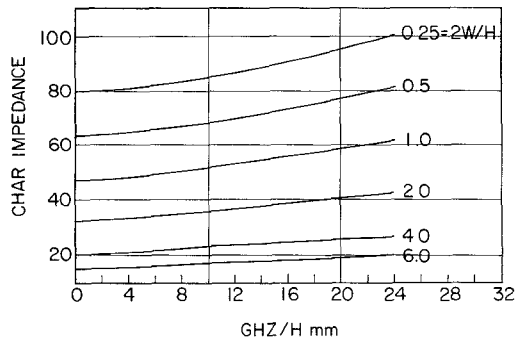

Fig. 5. Characteristic impedance with an Epsilam-10 substrate.

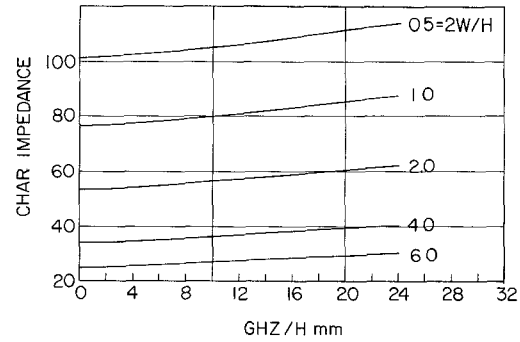

Fig. 7. Characteristic impedance with a boron nitride substrate.

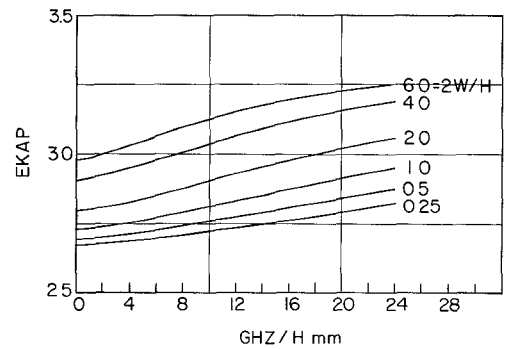

Fig. 6. Effective dielectric constant for boron nitride substrate.

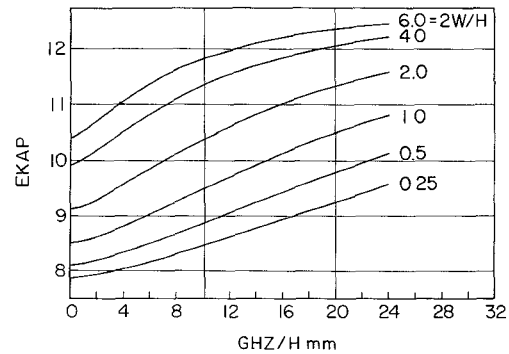

Fig. 8. Effective dielectric constant for GaAs substrate.

the numerical results obtained from the numerical implementation of the theory developed in this paper are accurate and reliable.

Fig. 2 shows the effective dielectric constant κ_e (called EKAP in the figures) for a sapphire substrate with $\kappa = 9.4$ and $\kappa_y = 11.6$ and several values of $2W/H$. Fig. 3 shows the corresponding characteristic impedance. The substrate thickness used in the computations was 1 mm, but the data can be applied for other thicknesses by scaling the frequency by the factor $1/H$, where H is the actual thickness in mm. For example, if $H = 0.5$ mm, the frequency in Figs. 2 and 3 cover the range 0 to 48 GHz.

The dispersion data for Epsilam-10 with $\kappa = 13$ and $\kappa_y = 10.3$ are shown in Figs. 4 and 5. At zero frequency and for $2W/H = 2$, we obtained $\kappa_e = 7.57$, $Z_0 = 32.20$. The corresponding values given by Alexopoulos [6, table III] are 7.54 and 32.16, which agree to better than 0.4 percent for κ_e and 0.15 percent for Z_0. For $2W/H = 9$, the results given by Alexopoulos for κ_e is 3.7 percent lower than ours. For an isotropic substrate with $\kappa = 10.3$, our results again are from 0.6 to 3 percent higher than those given by Alexopoulos depending on the strip width. Our values for the characteristic impedance are also slightly larger but the difference is less than 1 percent. It should be noted that the results given by Alexopoulos are for the case of a conducting shield a distance $9H$ above the substrate. When the shield is moved to a distance of $500H$ above the substrate, the results are in agreement with ours [19]. Pozar has also verified some of our computed results [20].

Figs. 6 and 7 give dispersion data for boron nitride with $\kappa = 5.12$ and $\kappa_y = 3.4$. The dielectric constant of GaAs has been measured as 12.9 at a wavelength of 5 mm [21]. Dispersion data for GaAs using $\kappa = 12.9$ are shown in Figs. 8 and 9. Alumina has a dielectric constant in the range 9.6 to 10.1 depending on composition. A typical quoted value is 9.7 for alumina in the microwave band [22], although measurements on alumina 995 at 60 GHz show a value of 9.6 [23]. We have used a value of 9.7 to compute the dispersion data shown in Figs. 10 and 11.

Fig. 12 shows a plot of the effective dielectric constant EKAP versus the dielectric constant kappa of the substrate for three line widths and three frequencies, namely $2W/H = 0.5$, 2, and 6 and $f = 0$, 10, and 20 GHz with $H = 1$ mm. The relationships are, remarkably, almost linear and the slopes of the lines are almost equal (10–15 percent less at $f = 0$ and within a few percent at $f = 20$ GHz) to EKAP/kappa. This property may be used to obtain the effective dielectric constant for a given microstrip line and frequency with a substrate whose dielectric constant differs by several percent from that for which data are available. For example, with $2W/H = 2$, $f = 10$ GHz, and $\kappa = 10$, the computed value of κ_e is 7.98. From this information, we can estimate κ_e for a similar line at the same frequency but with an alumina substrate having $\kappa = 9.7$. The estimate is given by

$$\kappa_e = 7.98 - 0.3 \times (7.98/10) = 7.7406$$

which is within 0.1 percent of the computed value 7.733. A similar estimate at $f = 0$ gives $\kappa_e = 6.936$, which is very close to the computed value 6.946.

Even though a large number of papers have been published on microstrip dispersion, there are very little actual data that have been published. An extensive set of tables giving the effective dielectric constant, characteristic im-

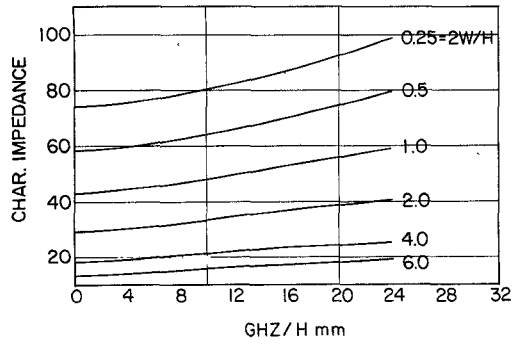

Fig. 9. Characteristic impedance with a GaAs substrate.

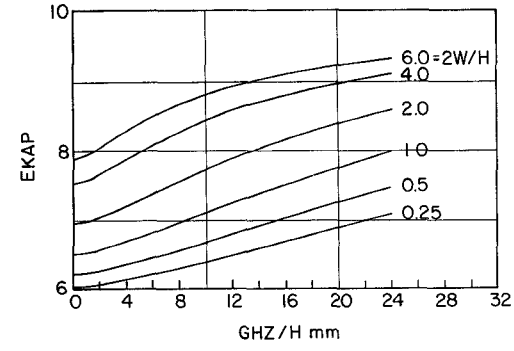

Fig. 10. Effective dielectric constant for alumina substrate.

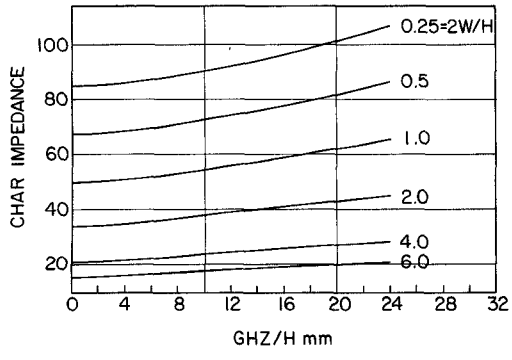

Fig. 11. Characteristic impedance with an alumina substrate.

pedance, and the current and charge expansion coefficients for a wide range of $2W/H$ values, substrate dielectric constants, and frequencies has been prepared [24]. The frequency range covered is 0 to 30 GHz for $H=1$ mm. Above 10 GHz, thinner substrates would normally be used and the frequency must be scaled accordingly by dividing by the actual value of H in mm that is used. For PTFE material filled with glass fiber or woven glass, the anisotropy ratios used were those given by Laverghetta [25]. The GW-BASIC program is also given in [24].

VII. Conclusions

A numerically efficient iteration-perturbation theory based on potential theory for analyzing microstrip dispersion was developed. The theory allows for anisotropic substrates. Since many substrate materials are anisotropic, it is important to include anisotropy if accurate design data are to be obtained. The theory was implemented by execution on a personal computer and will completely characterize a microstrip line in 2-GHz frequency increments from 0 to 30 GHz in less than 2 minutes. By using the INLINE CODE compiler and an 8087 coprocessor, the execution time is reduced by a factor of 2.4.

Work is currently under way to extend the method to slotlines and coupled microstrip and slotlines.

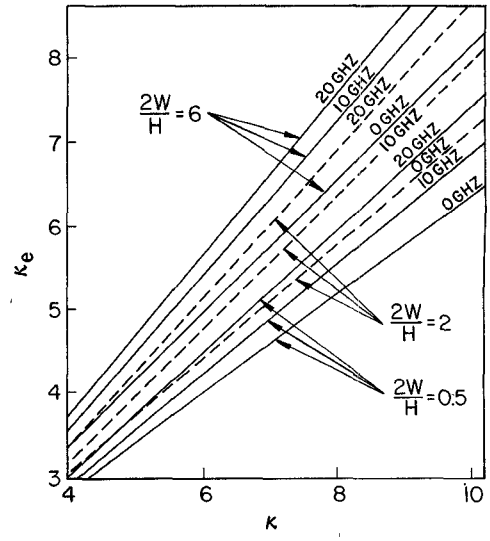

Fig. 12. Effective dielectric constant versus substrate dielectric constant.

References

[1] T. Itoh and R. Mittra, "Spectral domain approach for calculating the dispersion characteristics of microstrip lines," *IEEE Trans. Microwave Theory Tech.*, vol. MTT-21, pp. 496–499, 1973.

[2] R. H. Jansen, "High speed computation of single and coupled microstrip parameters including dispersion, high order modes, loss and finite strip thickness," *IEEE Trans. Microwave Theory Tech.*, vol. MTT-26, pp. 75–82, 1978.

[3] Y. Hayashi and T. Kitazawa, "Analysis of microstrip transmission line on a sapphire substrate," *J. Inst. Electron. Commun. Eng. Jap.* vol. 62-B, pp. 596–602, June 1979.

[4] T. Kitazawa and Y. Hayashi, "Propagation characteristics of striplines with multilayered anisotropic media," *IEEE Trans. Microwave Theory Tech.*, vol. MTT-31, pp. 429–433, June 1983.

[5] N. G. Alexopoulos and C. M. Krowne, "Characteristics of single and coupled microstrips on anisotropic substrates," *IEEE Trans. Microwave Theory Tech.*, vol. MTT-26, pp. 387–393, June 1978.

[6] N. G. Alexopoulos, "Integrated-circuit structures on anisotropic substrates," *IEEE Trans. Microwave Theory Tech.*, vol. MTT-33, pp. 847–881, 1985.

[7] R. H. Jansen, "The spectral-domain approach for microwave integrated circuits," *IEEE Trans. Microwave Theory Tech.*, vol. MTT-33, pp. 1043–1056, 1985.

[8] A-M.A. El-Sherbiny, "Hybrid mode analysis of microstrip lines on anisotropic substrates," *IEEE Trans. Microwave Theory Tech.*, vol. MTT-29, pp. 1261–1265, 1981.

[9] Y. Fujiki, Y. Hayashi, and M. Suzuki, "Analysis of strip transmission lines by iteration method," *J. Inst. Electron. Commun. Eng. Japan*, vol. 55-B, pp. 212–219, 1972.

[10] E. F. Kuester and D. C. Chang, "Theory of dispersion in microstrip of arbitrary width," *IEEE Trans. Microwave Theory Tech.*, vol. MTT-28, pp. 259–265, 1980.

[11] T. Itoh and R. Mittra, "Analysis of microstrip transmission lines," Antenna Lab., Univ. of Illinois, Urbana, Sci. Rep. No. 72-5, June 1972.

[12] B. E. Kretch, "Perturbation-iteration theory for analyzing microwave striplines," M.S. thesis, Case Western Reserve Univ., Cleveland, OH, Sept. 1985.

[13] B. E. Kretch, "Perturbation-iteration theory for analyzing microwave striplines," Electromagnetic Waves and Wave propagation Rep. WGR-85-5, Case Western Reserve Univ., Cleveland, OH, Sept. 1985.

[14] M. Kobayashi and R. Terakado, "New view on an anisotropic medium and its application to transform from anisotropic to isotropic problems," *IEEE Trans. Microwave Theory Tech.*, vol. MTT-27, pp. 769–775, 1979.
[15] R. E. Collin, *Field theory of Guided Waves*. New York: McGraw-Hill, 1960, p. 580.
[16] E. F. Kuester and D. C. Chang, "An appraisal of methods for computation of the dispersion characteristics of open microstrip," *IEEE Trans. Microwave Theory Tech.*, vol. MTT-27, pp. 691–694, 1979.
[17] J. L. Tsalamengas, N. K. Uzunoglu, and N. G. Alexopoulos, "Propagation characteristics of a microstrip line printed on a general anisotropic substrate," *IEEE Trans. Microwave Theory Tech.*, vol. MTT-33, pp. 941–945, 1985.
[18] R. P. Owens, J. E. Aitken, and T. C. Edwards, "Quasi-static characteristics of microstrip on an anisotropic sapphire substrate," *IEEE Trans. Microwave Theory Tech*, vol. MTT-24, pp. 499–505, Aug. 1976.
[19] N. G. Alexopoulos, private communication.
[20] D. M. Pozar, private communication.
[21] M. N. Afsar and K. J. Button, "Precise millimeter-wave measurements of complex dielectric permittivity and loss tangent of GaAs, Si, SiO_2, Al_2O_3, BeO, Macor, and glass," *IEEE Trans. Microwave Theory Tech.*, vol. MTT-31, pp. 217–223, 1983.
[22] Y. Tokumitsu, M. Ishizaki, M. Iwakuni, and T. Saito, "50-GHz IC components using alumina substrates," *IEEE Trans. Microwave Theory Tech.*, vol. MTT-31, pp. 121–128, 1983.
[23] M. N. Afsar, "Dielectric measurements of millimeter-wave materials," *IEEE Trans. Microwave Theory Tech.*, vol. MTT-32, pp. 1598–1609, 1984.
[24] R. E. Collin, "Microstrip dispersion-including anisotropic substrates," *Electromagnetic Waves and Wave Propagation Rep.* WGR-86-8, Case Western Reserve Univ., Cleveland, OH, Mar. 1986.
[25] T. Laverghetta, "Microwave materials: The choice is critical," *Microwave J.*, vol. 28, p. 163, Sept. 1985.

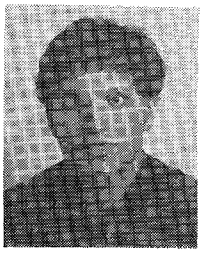

Brian E. Kretch (M'85) was born in Cleveland, OH, on October 3, 1960. He received the B.S. and M.S. degrees in electrical engineering and applied physics from Case Western Reserve University in 1982 and 1985, respectively.

Since 1985, he has been working at the IBM Corporation in Gaithersburg, MD, as an electrical engineer. His current areas of work include computer workstation systems development and computer workstation software development.

✠

Robert E. Collin (M'54–SM'60–F'72) received the B.Sc. degree in engineering physics from the University of Saskatchewan in 1951. He received the Ph.D. degree from Imperial College, University of London, in January 1954.

From 1954 to 1958, he was a Scientific Officer with the Canadian Armament Research and Development Establishment, Quebec. He joined the faculty at Case Institute of Technology in 1958 and became a Full Professor in 1965. He served as Chairman of the Electrical Engineering and Applied Physics Department from 1977 to 1982.

Dr. Collin is the author or coauthor of several books and numerous technical papers. He is a member of the USA URSI Commission B. He was an invited lecturer to the People's Republic of China in 1980, to the Catholic University in Rio de Janeiro in 1972 and 1986, and to the Telebras Research Center, Brazil, in 1986. He was a Distinguished Visiting Professor at Ohio State University in 1982–1983.